Catalysis Science & Technology

ROYAL SOCIETY OF CHEMISTRY

PAPER

View Article Online
View Journal | View Issue

Cite this: *Catal. Sci. Technol.*, 2026, **16**, 1238

Exploring the bimodal nature of a nickel-based catalytic system for the hydrogenation of alkenes and polycyclic aromatic hydrocarbons

Samuel Redl, [a] Simon Halas,[a] Uwe Monkowius [bc] and Christoph Topf *[a]

Received 10th November 2025,
Accepted 8th January 2026

DOI: 10.1039/d5cy01341k

rsc.li/catalysis

We communicate the syntheses, characterization, and catalytic application of a series of NHC-tagged nickel(II) half sandwich complexes (NHC = *N*-heterocyclic carbene). The described piano stool compounds function as precatalysts in the homogeneous hydrogenation of C=C bonds whereby the catalytic protocol is simple, robust, and additive-free. Moreover, one can opt between two modes both of which display distinguished catalytic features that can be exploited to achieve chemo- and regioselectivity. Mechanistic insights are provided with emphasis on the elucidation of the actual catalytically active species and, for the first time, we report on the formation of a hydride-bridged, dinuclear Ni cluster which contains a peculiar, six-membered diaza-nickelacycle. This compound resulted from oxidative addition of an NHC-related C–N bond onto a Ni moiety and this process is likely to represent a general deactivation mode for pertinent nickel catalysts.

Introduction

Catalytic hydrogenation is an indispensable tool for the chemical industries as this technology provides atom-efficient access to commodities and intermediates which are used for the manufacture of many important products including pharmaceuticals, dyes, agrochemicals, or aesthetically pleasing scents.[1–3] Typically, the addition of gaseous H_2 to organic molecules is achieved through the use of platinum group metals (PGMs). However, economic and scarcity issues associated with these noble elements have spurred the development of hydrogenation catalysts based on non-precious metals.[4] In this context, nickel is a suitable candidate due to its excellent abundance, low price, and propensity to form redox active hydrides,[5] which is also manifest in the occurrence of Ni in native metalloenzymes.[6,7]

One of the most prominent catalysts is spongy RANEY® Ni (ref. 8) albeit that its use entails meticulous lab-technical precautions[9] and the corresponding catalytic transformations often suffer from limited selectivities.[10] In order to remedy these issues, more robust and user-friendly composite materials were devised. These are usually prepared through controlled pyrolyses of a molecularly well-defined solution phase precursor that has been immobilized on supports such as carbon[11] or silica[12–15] prior to heat treatment. Yet, support-free approaches for the preparation of related, solid hydrogenation catalysts also exist.[16]

Next to working Ni into heterogeneous formulations, making soluble coordination compounds is a further proper means for achieving catalytic hydrogen transfer with this transition metal.[17] Early examples date back to the late 1960s when methyl linoleate and methyl oleate were hydrogenated with plain Ni–PPh_3 complexes.[18] Later, bidentate phosphines were shown to enable the efficient hydrogenation of 1-octene[19–21] and the privileged PNP pincer motif gave rise to related catalysts for the hydrogenation of C=C bonds, too.[22,23] Nickel complexes containing classic *N*-heterocyclic carbenes[24] (NHC) as well as analogous silylenes[25,26] and silyl ligands[27] complement this list. Moreover, N-donor ligands such as phosphoranimides[28] and Schiff bases[29] are well-suited for the design of catalysts that facilitate the reduction of olefins with molecular hydrogen. Very interestingly, the activation of H_2 is also possible at Ni–M interfaces (M = B, Al, Ga, or In)[30–32] and even Mg-based metalloligands cleave the strong H–H (ref. 33) or D–D (ref. 34) bond, respectively. Most importantly, Ni-based coordination compounds that incorporate enantiopure phospholanes[35] or chiral-at-P phosphines[36] allow for the asymmetric reduction of C=C bonds.

With respect to C≡C, the selective semihydrogenation of alkynes with several Ni/phosphine combinations[37–39] including an Si-based pincer ligand[40] has been reported. In addition, a Ni-gallylene motif was exploited to achieve the same catalytic transformation.[41]

Now, in order to expand upon our research program on hydrogenation catalysts derived from group 6 metal half sandwich complexes,[42,43] we embarked on a study towards

[a] *Institute of Catalysis (INCA), Johannes Kepler University (JKU), Linz 4040, Austria. E-mail: christoph.topf@jku.at*
[b] *Linz School of Education, Johannes Kepler University (JKU), Linz 4040, Austria*
[c] *Institute of Inorganic Chemistry (JKU), Linz 4040, Austria*

the development of structurally related organonickel species. For that purpose, compounds of the general formula [Ni(η^5-Cp)(NHC)X] (X = Cl, Br) fit well by virtue of their ready accessibility.[44–48] We chose NHCs as these compounds have emerged as a highly versatile ligand class in catalysis[49] since the isolation of the first stable carbene.[50] Furthermore, we wanted to bypass problems associated with the air sensitivity of phosphines which often interferes with the catalytic activity of pertinent complexes.[51]

Occasional reports on the catalytic capabilities of [Ni(η^5-Cp)(NHC)]-based coordination compounds have been published in the context of P_4 activation,[52] hydroboration,[53] and hydrosilylation.[54–56] In the context of hydrogenation, olefin-tethered complexes [Ni(η^5-Cp)(NHC)X] (X = Cl, Br) were employed as precursors for the preparation of NHC-tagged nanoparticles which function as a catalysts in various hydrogenation reactions.[57–59] Yet, to the best of our knowledge, an atom-efficient, homogeneous(-like) method for the reduction of C=C bonds relying on Ni-derived piano stool complexes has not been reported so far. Herein, we present a flexible and user-friendly catalytic protocol which deploys gaseous H_2 as the principal reductant and that dispenses with the need for any companion reagents such as strong bases or moisture-sensitive hydrides.

Results and discussion

Catalytic pretests and optimization studies

Initially, we probed a series of NHC-tagged piano stool chlorides **[Ni] 1–5** for their ability to function as precatalysts in the hydrogenation of alkenes (Table 1). The conversion of cyclooctene **1a** into cyclooctane **2a** was chosen as a standard of comparison and in order to convert the Cl complexes into the corresponding hydrides, which are supposed to actually promote the hydrogenation process, the benchmark reaction

Table 1 Precatalyst testing for the pressure hydrogenation of alkenes

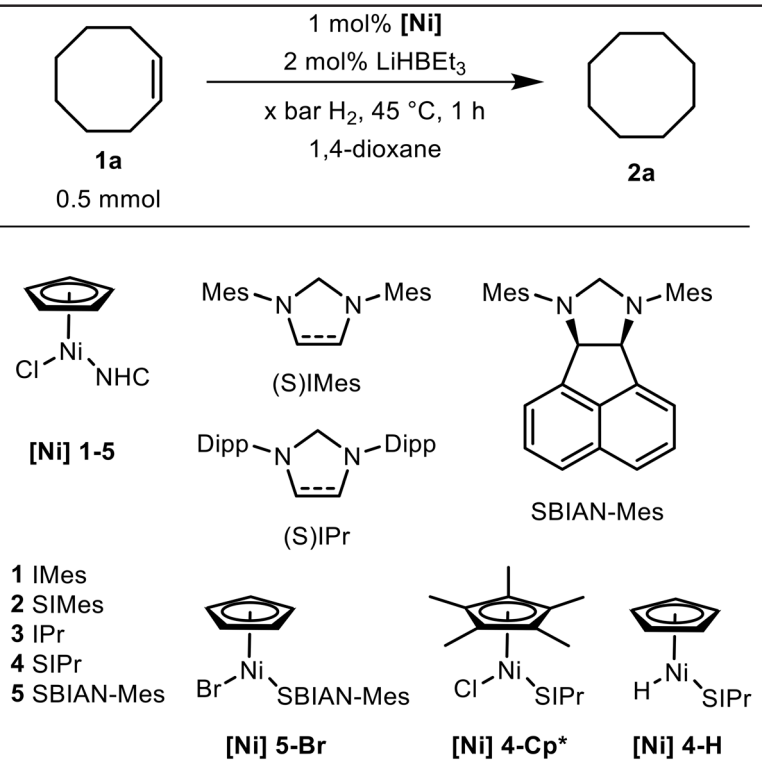

Entry	[Ni] precursor	p H_2/bar	Conv.[a]/%
1	**[Ni] 1**	20	15
2	**[Ni] 2**	20	25
3	**[Ni] 3**	20	>99
4	**[Ni] 4**	20	>99
5	**[Ni] 5**	20	88
6	**[Ni] 5-Br**	20	61
7[b]	**[Ni] 4-Cp***	20	>99
8	**[Ni] 3**	5	22
9	**[Ni] 4**	5	34
10	**[Ni] 4-H**, no $LiHBEt_3$	20	>99

[a] Determined by means of GC-MS analyses (*n*-hexadecane served as the internal standard). [b] The addition of $LiHBEt_3$ prompted the formation of the 17e species [Ni(η^5-Cp*)(SIPr)].

was conducted in the presence of an auxiliary reagent ($LiHBEt_3$). We found that the activity of the complexes strongly depends upon the NHC's wingtip substituents, *i.e.*, the Dipp-bearing (Dipp = 2,6-diisopropylphenyl) complexes (**[Ni] 3**, **[Ni] 4**) performed best and enabled complete substrate conversion whereas the Mes-substituted (Mes = 2,4,6-trimethylphenyl) congeners (**[Ni] 1**, **[Ni] 2**) seriously lagged behind (entries 1–4). Moreover, the degree of saturation in the imidazole-derived portion of the NHC proved to be relevant: imidazoline-based moieties (SIMes and SIPr) gave rise to more active catalysts compared to their imidazole counterparts (IMes and IPr) which still contain a C=C bond in the 4,5-position. The effect became evident when the hydrogenation experiment was run at lower H_2 pressure, *i.e.*, 5 *vs.* 20 bar (entries 8 and 9). The large discrepancy in activity between **[Ni] 2** and **[Ni] 4** can be attributed to cluster formation that forestalls the hydrogenation process (*vide infra*). The bis(imino) acenaphthene-derived carbene SBIAN-Mes[60,61] motif seems to curb the catalyst deactivation associated with the Mes groups but still this precatalyst could not compete with ones containing the standard Dipp-substituted NHCs (entry 5).

In order to render the transformation **1a** → **2a** additive-free, we first synthesized the hydride **[Ni] 4-H** in a separate step and applied it directly without any companion reagent and, rewardingly, we were able to reproduce the result obtained with the **[Ni] 4**/$LiHBEt_3$ *in situ* system (entry 10). Interestingly, treatment of congeneric **[Ni] 4-Cp*** with $LiHBEt_3$ did not yield a hydride but gave the paramagnetic, 17e species **[Ni(η^5-Cp*)SIPr]** instead. Yet, the latter performed excellent in the model reaction (entry 7) but since paramagnetic species often obstruct mechanistic investigations, especially with regard to NMR spectroscopy, we focused on Cp complexes that were diamagnetic, 18e complexes.

Since isolable **[Ni] 4-H** is a fairly stable, 18e complex, we reasoned that this is not the true catalyst that brings about the alkene hydrogenation. Thus, in order to generate the notional active species, **[Ni] 4-H** was first subjected to an H_2 atmosphere (45 °C, 20 bar) for 3 h whereupon **1a** was added to the reaction solution (Table 2). Strikingly, substrate conversion was complete within only 5 min and without the preactivation step, 1 h was necessary to fully convert cyclooctene (entries 1 and 3). To our delight, once **[Ni] 4-H** had been activated, the conversion **1a** → **2a** took place under very mild reaction conditions (5 bar H_2, RT) and even under 1 bar H_2 albeit longer reaction times were necessary to achieve meaningful conversions (entries 8 and 10). Importantly, both preactivation and cyclooctene hydrogenation were, not at all, hampered by the presence of Hg which points towards an authentic, homogeneous hydrogenation pathway (entry 2).

Furthermore, we established that catalyst formation is strongly affected by the nature of the alkene: on using non-activated **[Ni] 4-H** and 1-octene, the entire hydrogenation process was sluggish and only a minor fraction of the olefin was converted. However, when a preactivated sample of **[Ni] 4-H** was applied, hydrogenation of the same terminal alkene was again possible within a very short period of time (entries 4 and 5). It turned out that if the terminal olefin is present from the outset, a considerably stable bis(alkene) complex is formed that obstructs the generation of the active species (*vide infra*). On the other hand, the alkene does not impede the catalytic transformation if **[Ni] 4-H** is activated prior to olefin addition.

Table 2 Control experiments under preactivation conditions

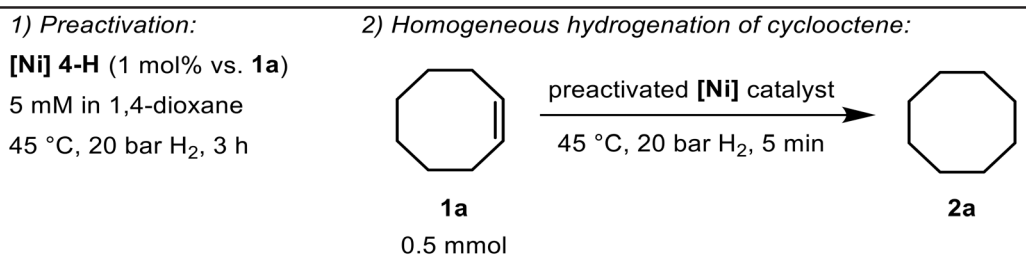

Entry	Deviation from the standard procedure	Conv.[a]/%
1	None	>99
2[b]	Hg drop test	>99
3	No preactivation step, 1 h in step 2)	>99
4	No preactivation step, 1 h in step 2), 1-octene instead of cyclooctene in step 2)	<10
5	1-Octene served as the substrate in step 2)	>99
6	**[Ni] 2-H** (SIMes) instead of **[Ni] 4-H** (SIPr)	26
7[c]	**[Ni 4]**/$LiHBEt_3$ instead of **[Ni] 4-H**	>99
8	5 bar H_2, RT, and 1 h were applied in step 2)	>99
9	As in entry 8, but 5 bar H_2 in step 1)	16
10	1 bar H_2, RT, and 1 h were applied in step 2)	40

[a] Determined by means of GC-MS analyses (*n*-hexadecane served as the internal standard). [b] 150 equiv. of liquid mercury *vs.* **[Ni] 4-H** were added. [c] 2 equiv. of $LiHBEt_3$ *vs.* **[Ni] 4** were added.

Mechanistic studies

Hydrogenation of **[Ni] 4-H** in THF-d_8 gave a complex ^{1}H NMR spectrum with various hydride signals in the high-field range, *i.e.*, from −4 to −26 ppm (Fig. 1A) including the one of remaining **[Ni] 4-H** at −23.6 ppm. The COSY plot shows three mutually coupled hydrides that are associated with the active species as these signals vanish upon addition of cyclooctene; however new hydridic signals emerged (SI). In the reaction mixture, we also detected cyclopentane which was presumably formed through expulsion of CpH from the Ni precatalyst followed by hydrogenation of the C=C bonds thus leaving behind a [Ni(0) NHC] unit. Notably, a similar route for the formation of a NHC-tagged Ni(0) species was previously reported in the context of

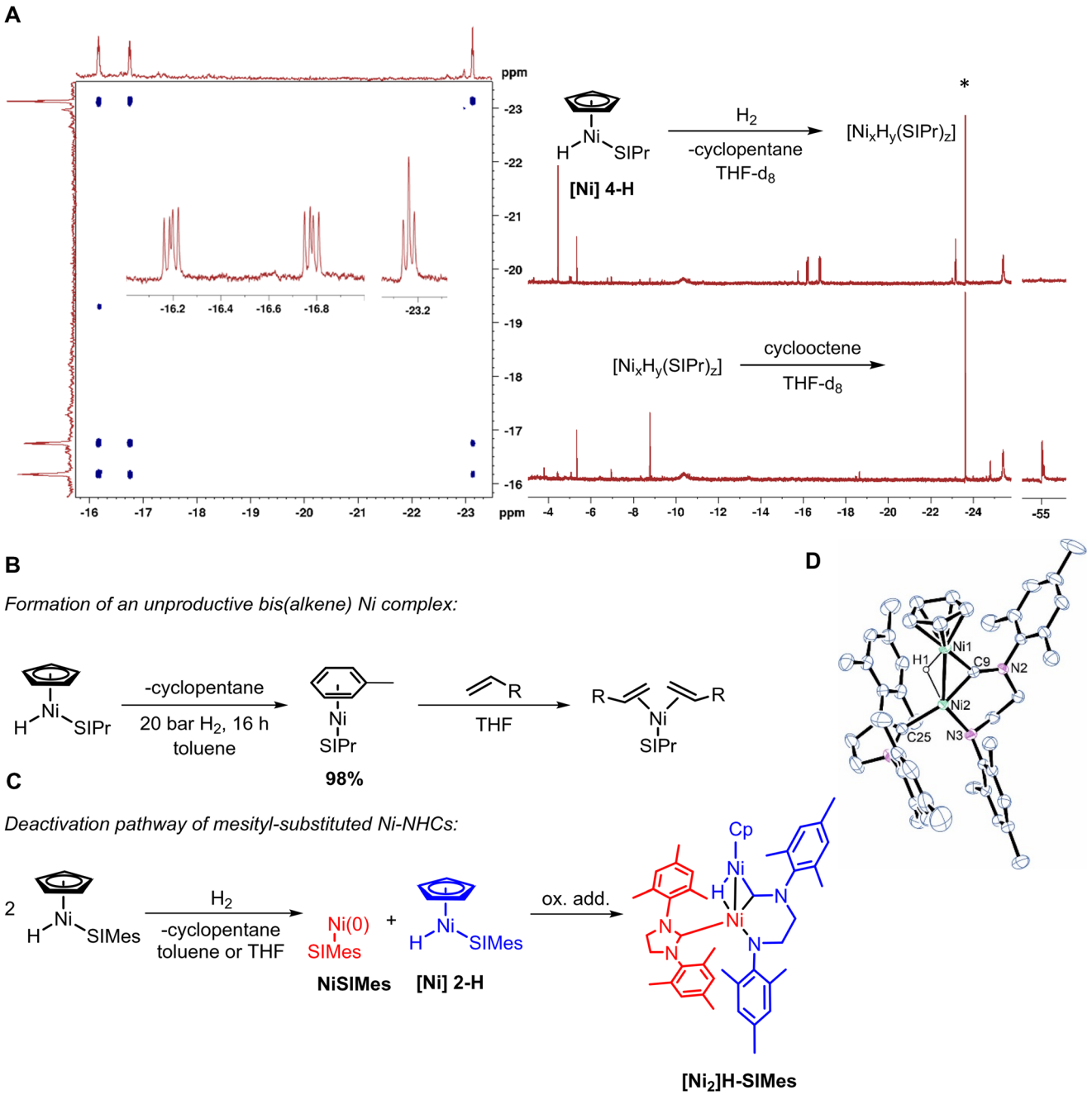

Fig. 1 (A, left) ^{1}H COSY NMR spectrum of a hydrogenated sample of **[Ni] 4-H** in THF-d_8 highlighting the hydridic region. (A, right) Excerpt of the ^{1}H NMR spectrum of hydrogenated **[Ni] 4-H** before and after the addition of cyclooctene showing the emergence of new hydride species; *hydride signal of unreacted precursor **[Ni] 4-H**. (B) Hydrogenation of **[Ni] 4-H** in toluene furnished stable [Ni(0)(SIPr)(η^6-toluene)] that afforded a fairly unreactive bis(alkene) complex upon reaction with a terminal, aliphatic olefin. (C) Hydrogenation of kindred **[Ni] 2-H** produced the unusual cluster compound **[Ni_2]H-SIMes** by way of oxidative addition. (D) Molecular structure of **[Ni_2]H-SIMes** as determined by SC-XRD analysis; all hydrogen atoms, except for the bridging hydride, were omitted for brevity.

C–H activation.[62] The invoked Ni carbene is then likely to aggregate into a polyhydride cluster [$Ni_xH_Y(SIPR)_z$] that displays hydrogenation capabilities in its own right. Since a catalytically active, phosphine-tagged polynuclear Ni complex has already been described in the literature, the existence of NHC analogs is reasonable.[63] Very recently, *in situ* formed, soluble Ni-nanoclusters were identified as the active species in the unusual geminal dihydroboration of alkynes.[64] Just like in our case, the higher nuclearity of the catalyst enables unprecedented reactivity, demonstrating the potential that lies beyond the traditional binary classification into homogeneous and heterogeneous catalysis.

As free [Ni(0)NHC] complexes are not stable and tend to form higher aggregates[65] we performed the **[Ni] 4-H** hydrogenation in toluene to intercept the pertinent carbene complex as stable **[Ni(0)(SIPr)(η^6-toluene)]** (Fig. 1B).[66] If not prohibited by steric hindrance, aliphatic alkenes may substitute for the arene to yield 16e bis(alkene) complexes.[67,68] The ability of NHC-tagged motifs to form such intermediates thus provides a rationale for the fact that some olefins are hydrogenated at slower rates compared to standard cyclooctene especially when the alkene is already present next to unactivated **[Ni] 4-H** (Table 2, entry 4).

Note that the reduction of **[Ni] 4-H** with gaseous H_2 is a robust alternative to [$Ni(COD)_2$]-based approaches for the preparation of [Ni(arene)(NHC)] complexes that serve as convenient Ni carbene synthons.

Next, the SIMes congener **[Ni] 2-H** was hydrogenated and, to our surprise, we found that its imidazoline moiety did not maintain its integrity but underwent ring expansion to afford a hitherto unknown nickelacycle that dominates the structure of the formed cluster **[Ni_2]H-SIMes** (Fig. 1C). The constitution of the H-bridged, dinuclear complex was confirmed by SC-XRD analysis (Fig. 1D) together with ^{1}H NMR spectroscopy. In light of the fact that imidazole-based NHCs are generally seen as inert spectator ligands, the oxidative addition of the pertinent C–N bond onto [Ni(0)(SIMes)] is a remarkable result. Interestingly, the cluster formation is independent of the solvent and any attempts at isolating [Ni(0)(SIMes)(η^6-toluene)], in order to intercept the elusive [Ni(0)(SIMes)] fragment, failed.

Note that our experimental findings are reminiscent of a recent report dealing with the synthesis and characterization of a cyclic Fe carbyne complex.[69] In that case, a C–S bond of a 4-thiazoline core underwent oxidative addition to furnish the corresponding six-membered metallacycle.

Importantly, **[Ni_2]H-SIMes** is not a self-contained catalyst but still, its formation is not a dead end: keeping the cluster under an atmosphere of H_2 at elevated temperature, catalytic activity is regained (SI). In that sense, the cluster generation is just a temporary deactivation process.

Next, we looked into the interaction between different alkene substrates and [Ni(0)(SIPr)(η^6-toluene)] which can be viewed as an arene-stabilized version of the fugacious (but very crucial) [Ni(0)(SIPr)] unit. Treatment of the Ni(arene) complex with excess cyclooctene $\mathbf{L_i}$ (4 equiv.) in THF-d_8 caused full displacement of toluene upon which the proton resonances of the associated $\mathbf{L_i}$ moiety appeared as a set of three broad signals shifted upfield compared to free cyclooctene (Fig. 2A) thus indicating a chemical exchange process. Since broad coalescence between coordinated and free $\mathbf{L_i}$ is observed, the magnitude of the exchange rate k is similar to that of the complexation-induced shift (CIS) $\Delta\nu$.[70,71] As an aside, the latter is exceptionally large for complexes of the type [Ni(0)(alkene)$_2$NHC] by virtue of strong backdonation from the Ni center into the antibonding alkene's π^* orbital.[24,67,72] In case of Ni-bound $\mathbf{L_i}$, the protons directly attached to the C-sp^2 atoms experience the largest broadening while that of the other H atoms pertaining to cyclooctene decreases as the distance to the C=C bond increases. Concurrently, all H signals associated with the SIPr ligand appear as sharp lines since they all fall into the fast exchange regime ($k > \Delta\nu$).

Concerning the number of cyclooctenes that coordinate to the [Ni(SIPr)] fragment, we refer to previously published calculations that were performed on [Ni(COD)(SIPr)] (COD = 1,5-cyclooctadiene).[73] These showed that COD solely bonds in the η^2 mode and the formation of the bis-COD congener [Ni(η^2-COD)$_2$(SIPr)] is strongly hampered due to steric constraints; for the same reason, the isomer [Ni(η^2,η^2-COD)(SIPr)] cannot form. Hence, given the great similarity of COD and $\mathbf{L_i}$, we used this computational study to argue that the equilibrium [Ni($\mathbf{L_i}$)(SIPr)] + $\mathbf{L_i}$ $\rightleftarrows$ [Ni($\mathbf{L_i}$)$_2$(SIPr)] takes place whereat the left side of the reaction equation is favored.

By contrast, reaction of [Ni(SIPr)(η^6-toluene)] with 1-octene $\mathbf{L_t}$ (4 equiv.) produced well-defined signal sets for the free and coordinated olefins of the ^{1}H NMR spectrum (Fig. 2A). This indicates that any exchange processes between free and coordinated alkene are slow compared to when cyclooctene is present (*vide supra*). Furthermore, the analogous reaction [Ni($\mathbf{L_t}$)(SIPr)] + $\mathbf{L_t}$ $\rightleftarrows$ [Ni($\mathbf{L_t}$)$_2$(SIPr)] is now clearly biased towards the right side (quantitative formation of [Ni($\mathbf{L_t}$)$_2$(SIPr)] according to ^{1}H NMR) because $\mathbf{L_t}$ can avoid steric clash as terminal olefins are more flexible than internal ones. Hence, the formation of the congested, but rather stable, 16e species [Ni($\mathbf{L_t}$)$_2$(SIPr)] becomes feasible. The latter also reinforces the fact that 1-octene's hydrogenation rate is drastically reduced compared to cyclooctene (Table 2, entry 4) since, obviously, the bis(alkene) complex is more stable presumably due to stereoelectronic effects. Yet, it has to be mentioned here, that Ni-promoted activation of H_2 is also possible on crowded 16e species as shown by Moret and coworkers. In their study, an olefin-substituted diphosphine complex was shown to heterolytically cleave H_2 by way of cooperation between the alkene tether and the Ni center;[39] similar activation pathways could also exist for related NHC complexes.

The kinetic profiles for the hydrogenation of cyclooctene and 1-octene reflect their different coordination behavior (Fig. 2B). On using precatalyst **[Ni] 4-H** in 1,4-dioxane, cyclooctene was fully converted within 45 min (black trace) whereas the reduction of 1-octene was sluggish, *i.e.*, only 60% conversion were achieved after 6 h (green trace). This

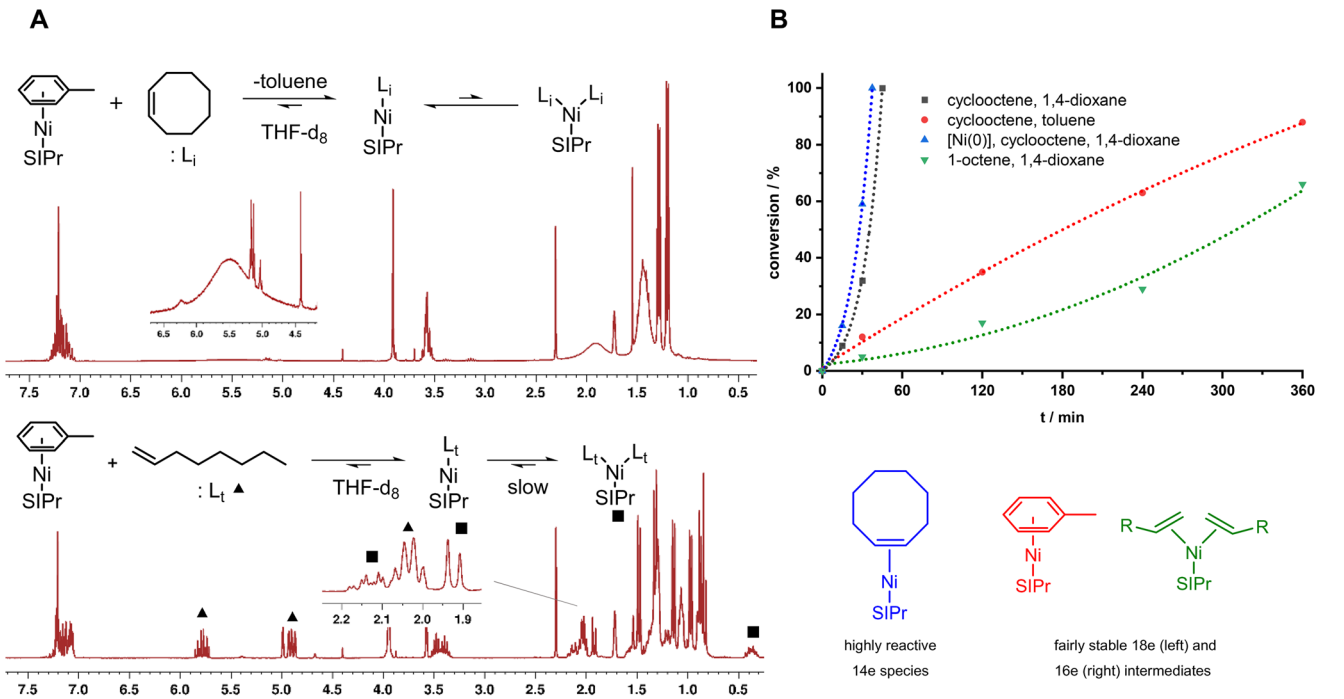

Fig. 2 (A, top) Displacement of η^6-coordinated toluene through reaction with cyclooctene (L_i); the line broadening in the ^1H spectrum is due to exchange between free and bound L_i. (A, bottom) reaction between 1-octene (L_t) and [Ni(0)(SIPr)(η^6-toluene)] yields relatively stable [Ni(0)(L_t)$_2$(SIPr)]; in this case, dynamic behavior is not observed on the NMR time scale. (B) Conversion-time diagram showing the influence of substrate and solvent on the catalytic hydrogenation's rate. The indices i and t stand for 'internal' and 'terminal', respectively. Conditions: 0.5 mmol substrate, 1 mol% **[Ni] 4-H**, 1.0 ml solvent, 20 bar H_2, 45 °C. [Ni(0)] refers to [Ni(0)(SIPr)(η^6-toluene)].

observation is in agreement with the presence of the more reactive, 14e species [Ni($\mathbf{L_i}$)(SIPr)] and less reactive, sterically congested 16e intermediate [Ni($\mathbf{L_t}$)$_2$(SIPr)]. Importantly, the kinetic curve for the catalytic transformation conducted with [Ni(SIPr)(η^6-toluene)] in the same solvent (blue trace) parallels that of the experiment that was run with **[Ni] 4-H**. This indicates that both routes proceed through a common intermediate that actually sustains the catalytic cycle, *i.e.*, [Ni(SIPr)]. This assertion is supported by the fact that cyclooctene reduction is severely hampered if performed in toluene (red trace). In this case, any free [Ni(SIPr)] is immediately captured as the stable, 18e complex [Ni(SIPr)(η^6-toluene)] which is not a catalyst on its own. Note that this finding also underlines that benzene-derived solvents are not the ideal choice for hydrogenations promoted by Ni–NHCs since they readily form stable intermediates with the solvent that impede the catalytic hydrogenation process as a whole.[24]

Substrate scope and limitations

Building upon the initial catalytic experiments we established a protocol for olefin hydrogenation that relies on the substrate-coordinating mononuclear [Ni(NHC)] motif (mode I, Scheme 1, left column) and one that rests on the formation of rather ill-defined polyhydride clusters [Ni$_x$H$_Y$(SIPR)$_z$] (mode II, Scheme 1, right column). Generally, mode I is apt for the reduction of internal alkenes whereas terminal ones are better accommodated by mode II. Notably, when we first applied mode I to *cis*-stilbene **1s** and the conjugated diene **1v** we observed substantial byproduct formation due to partial or full hydrogenation of the Ph rings. However, on using mode II, the formation of unwanted side products was effectively curbed. Note that bicyclic norbornene **1u** is a substrate on which mode I performed only poorly. Although being an internal alkene, **1u** presumably forms a fairly stable complex by virtue of its compact shape.

In the case of α,β-unsaturated ketones, we found that the conjugated C=C bond in benzylidene acetone **1e** was preferably reduced thus leaving the carbonyl group mostly intact. Yet, in *trans*-chalcone **1f** where the Me group is substituted for a Ph substituent the C=O group was hydrogenated to produce the corresponding secondary alcohol. Concerning the conjugated esters **1g–i**, the catalytic conversion was selective in that the C=C bond next to the ester group was reduced while the CO_2R motif itself remained untouched. Diethyl fumarate **1j** was unreactive owing to the formation of stable [Ni(fumarate)$_2$NHC].[74] Preactivation of the catalyst did not lead to any significant improvement in this case. Rewardingly, mode I copes with steric bulk such that the trisubstituted cinnamate derivative **1i** was neatly converted into the wanted product. Interestingly, the same system was unable to fully convert simple cinnamaldehyde **1d** whereas challenging citral **1l** and geraniol **1m**, both of which contain two trisubstituted olefin moieties, were regioselectively reduced at the conjugated site and not at the periphery. However, tetrasubstituted alkene

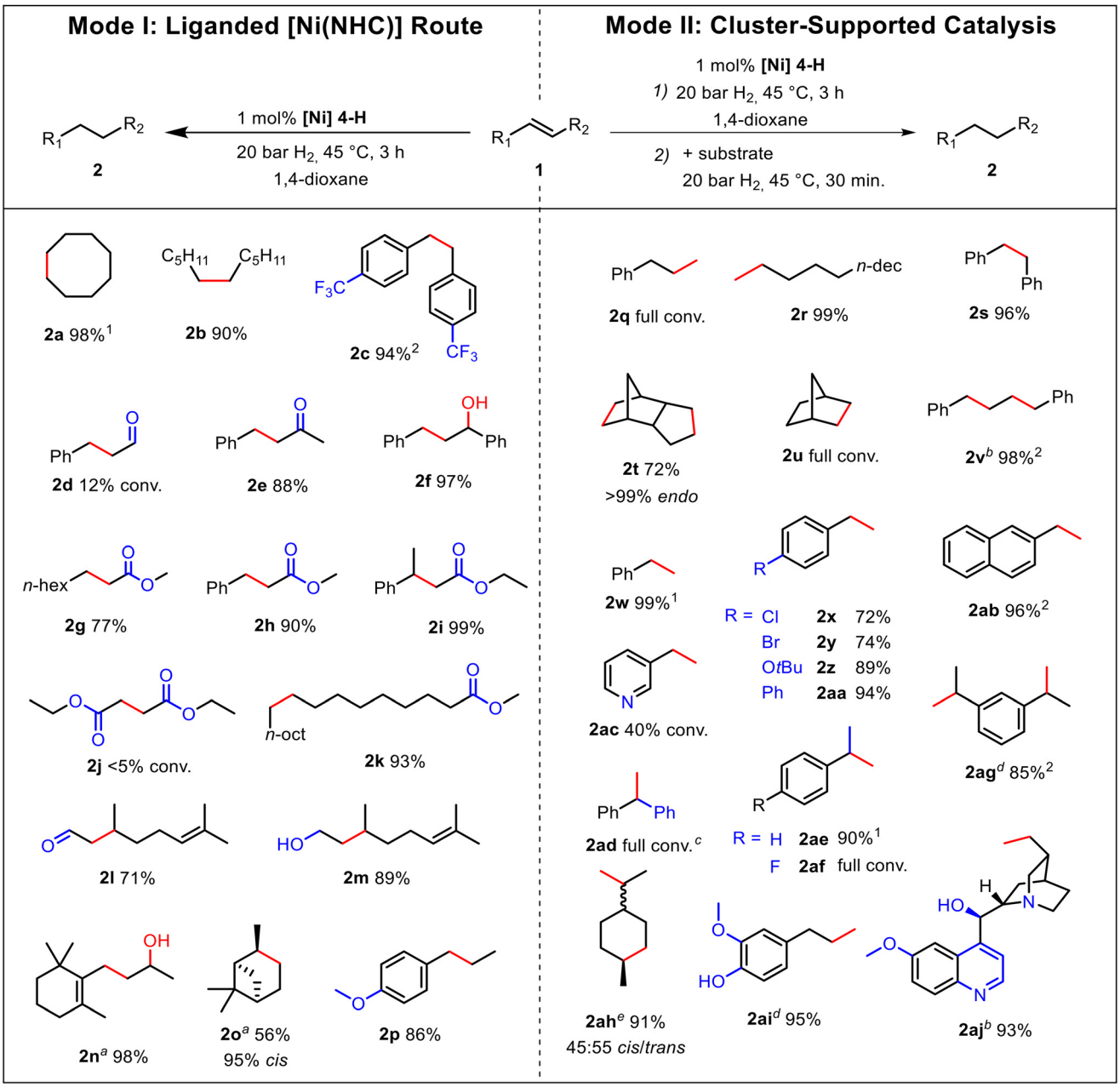

Scheme 1 Percentage values refer to isolated yields if not stated otherwise; [1]GC-MS yield (*n*-hexadecane served as the internal standard); [2]NMR yield (1,3,5-trimethoxybenzene served as the internal standard); [a]16 h reaction time; [b]3 h reaction time during 2); [c]mixture of products due to arene-hydrogenation; [d]2 mol% **[Ni] 4-H**; [e]2 mol% **[Ni] 4-H**, THF, and 3 h reaction time during 2).

motifs were not converted and β-ionone **1n** gave, accordingly, the alcohol that stems from reduction of the C=O group and the disubstituted C=C bond.

Mode II excels in the reduction of terminal alkenes and, gratifyingly, the catalytic transformation is not obstructed by deleterious oxidative addition that might occur in aryl halides **1x**, **1y**, and **1af**. Interestingly, under the conditions of mode I, α-methylstyrene **1ae** underwent exhaustive hydrogenation to produce isopropyl cyclohexane as the major product (>90%) whereas the cluster-supported approach was more selective and gave cumene almost exclusively. We attribute the exhaustive hydrogenation to a mechanistic pathway initiated by arene-coordination to [Ni(0)SIPr] and the alkene-activating effect (SI).[75] Hydrogenation of limonene **1ah** yielded a well-balanced diastereomeric mixture of *cis*- and *trans*-menthane and even a highly functionalized molecule such as quinine **1aj** was cleanly converted.

The hydrogenation of fused arenes (mode I) typically required forced reaction conditions (increased loading of **[Ni] 4-H**, higher temperature, and/or higher H_2 pressure) in order to achieve decent substrate conversions (Scheme 2). However, unsubstituted naphthalene and anthracene were partially

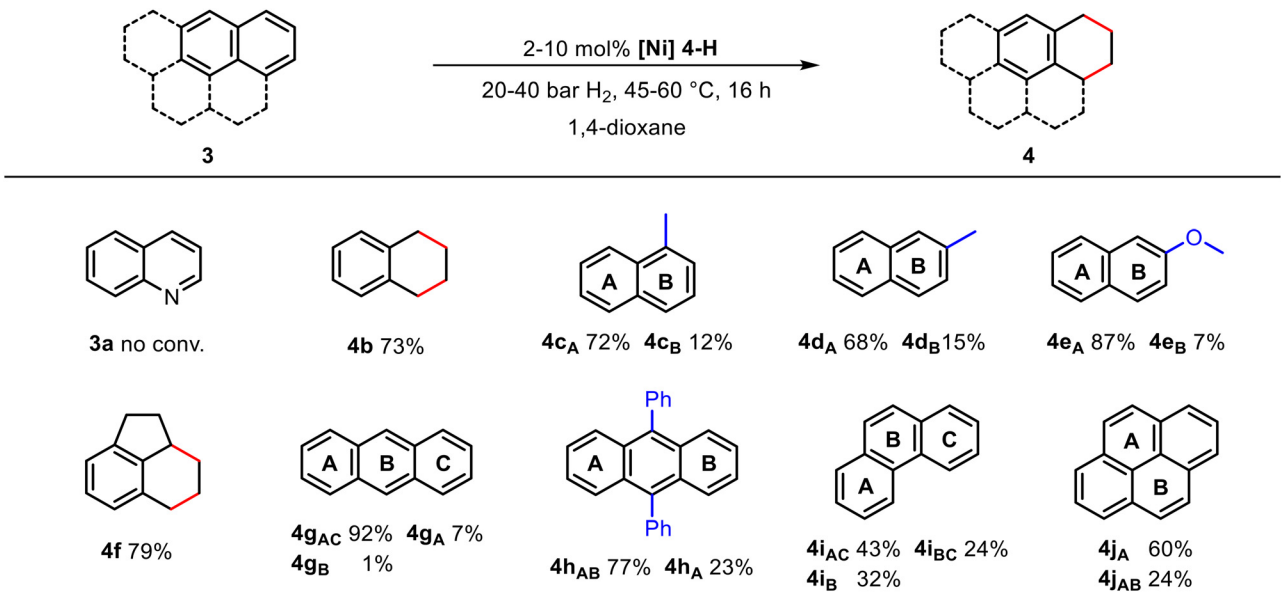

Scheme 2 Substrate scope for the hydrogenation of polycyclic aromatic hydrocarbons. 5 mol% of **[Ni] 4-H**, 40 bar H_2 and 45 °C were applied as standard conditions with the following adjustments: 2 mol% of **[Ni] 4-H** and 20 bar H_2 for **3b**, 10 mol% and 60 °C for **3i**, 60 °C for **3j**. With the exception of **4b**, products were isolated as a mixture and each yield was determined by means of ^{1}H NMR spectroscopy (1,3,5-trimethoxybenzene served as the internal standard). Capital letters indicate hydrogenated carbocycles.

reduced under comparably low precatalyst loading (2 mol% **[Ni] 4-H**) and H_2 pressure (20 bar). Under these conditions, anthracene was reduced mainly to tetrahydroanthracene. Applying the standard conditions gave $\mathbf{4g_{AC}}$ as the main product instead. Substituted naphthalenes required 5 mol% of the precatalyst and with respect to regioselectivity, we found that the unsubstituted moiety had been preferentially hydrogenated with selectivities ranging from 4.5 : 1 for **4d** to 12 : 1 for **4e**. Notably, phenanthrene and pyrene called for the harshest conditions (60 °C, 40 bar H_2) so as to achieve satisfying results. Hydrogenation of quinoline (**3a**) failed, most likely due to the stability of the dimer [(η^2-quinoline) Ni(SIPr)]$_2$.[65]

Miscellaneous and outlook

To expand upon the application range of our [Ni(NHC)]-based system, we tested preactivated **[Ni] 4-H** for its ability to promote chain walking isomerization since we frequently observed minor quantities of olefin isomers in the reaction mixture. Indeed, eugenol **1ai** was neatly converted into *trans*-isoeugenol **1ai′** at mild temperature (60 °C, Scheme 3A). This shows that the pertinent Ni–NHC can also be applied as a self-contained alkene isomerization catalyst.

Next, we wanted to know whether the one-coordinate [Ni(NHC)] catalyst ceases to work in the presence of excess carbene ligand. For that purpose, **[Ni(SIPr)(η^6-toluene)]** was first combined with SIPr to afford homoleptic **[Ni(SIPr)$_2$]** which was then applied to the hydrogenation of cyclooctene. Surprisingly, the bis(NHC) complex was still catalytically competent despite increased steric bulk and reduced vacancies at the Ni center. Then, **[Ni(SIPr)$_2$]** was used as a presumptive catalyst in the hydrogenation of 1-octene. The intention here was to forestall the detrimental formation of a bis(alkene) complex which was shown to impede the catalytic process (*vide supra*). To our delight, also this olefin was smoothly converted into the wanted alkane (Scheme 3B). Thus, using [Ni(SIPr)$_2$] offers an alternative way of reducing terminal alkenes without prior activation of **[Ni] 4-H** (mode II).

During the elaboration of the substrate scope, mode I enabled the hydrogenation of several prochiral substrates such as citral **1l**, α-pinene **1o**, and ethyl β-methyl cinnamate **1i** (Scheme 1). Adding ketones and ketimines makes an array of substrates, the asymmetric hydrogenation of which accesses interesting chiral building blocks (alcohols, amines, and saturated esters). Interestingly, we found that C═O and C═N bonds have also succumbed to catalytic hydrogenation effected by **[Ni] 4-H** (Scheme 3C). Since NHC ligands can be made chiral these important preliminary results open up new vistas for the development of base metal catalysts that enable enantioselective hydrogenation reactions.

Lastly, we wanted to ameliorate the selectivity towards the C═C bond in the conjugate reduction of enones (Scheme 3D). We hypothesized that an aldehyde additive could prevent the ketone motif from binding to the Ni core thus leaving it behind unaltered after the hydrogenation experiment. This approach was guided by the idea that the Ni(0)-catalyzed Tishchenko reaction, initiated by [Ni(aldehyde)$_2$(NHC)], might outcompete the formation of an oxanickelacycle *via* reaction between Ni(0)NHC and the ketone.[76,77] The latter is a plausible starting point for the hydrogenation of ketones with Ni(0)NHC as a catalyst. Indeed, we found that benzaldehyde effectively suppresses the reduction of the C═O group in *trans*-chalcone to exclusively afford the tagged

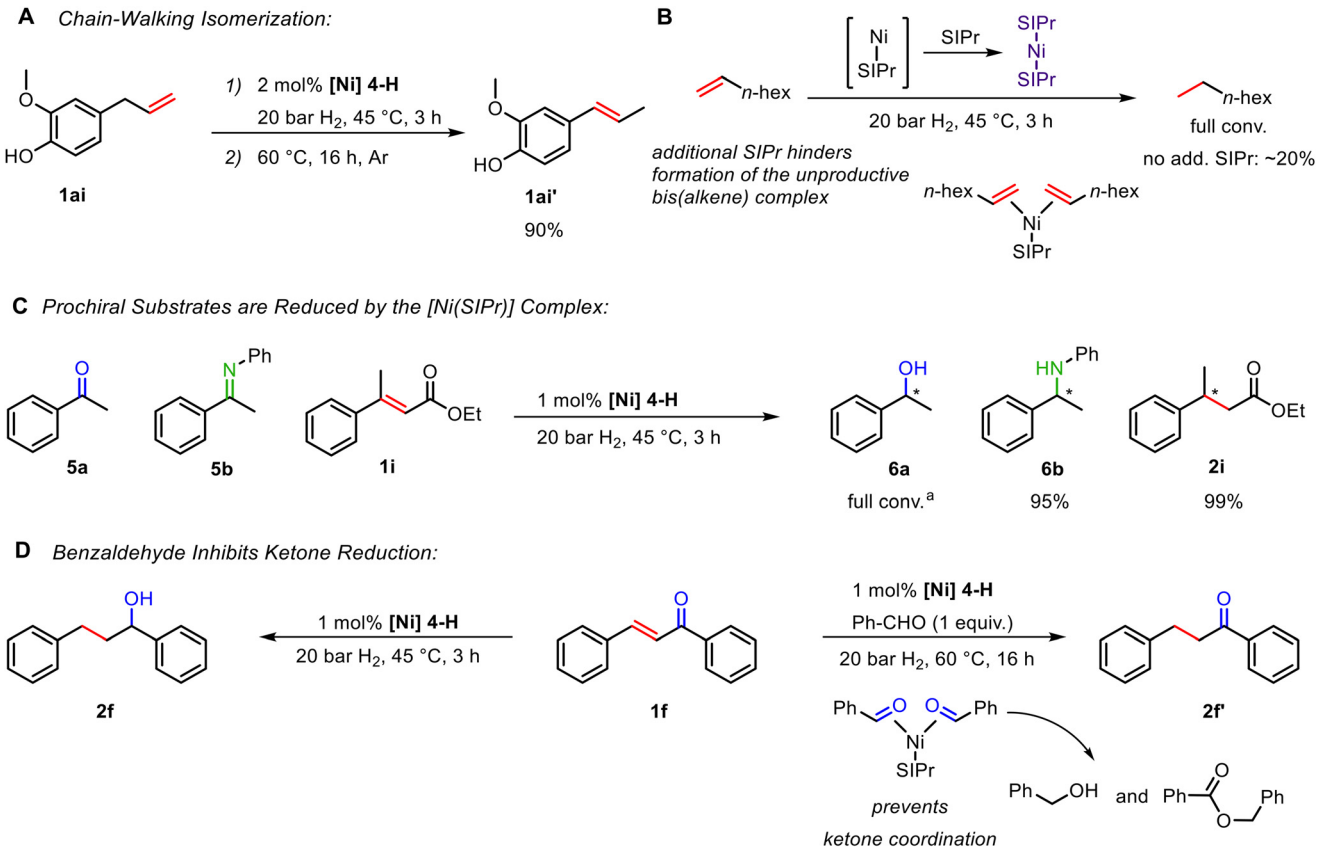

Scheme 3 Further applications and tunability of the catalytic system. (A) Isomerization of eugenol into *trans*-isoeugenol. (B) *In situ*-generated [Ni(SIPr)$_2$] functions as a more active catalyst for the hydrogenation of 1-octene compared to **[Ni(0)(SIPr)(η^6-toluene)]**. (C) Ni-catalyzed hydrogenation of prochiral substrates into racemic products; [a]16 h reaction time. (D) Deliberate catalyst poisoning with benzaldehyde to circumvent the reduction of the ketone motif in *trans*-chalcone.

ketone **2f'**. Incidentally, benzaldehyde ended up as benzyl alcohol and benzyl benzoate as the homocoupling product.[76]

Conclusions

We established a general, [Ni(SIPr)]-based catalytic protocol for the homogeneous hydrogenation of olefins. An analogous, SIMes-derived catalyst furnishes a peculiar, six-membered nickelacycle that represents a temporarily deactivated state which can be reactivated under an atmosphere of H_2. The SIPr-based system is more flexible and can be used in two ways. The first mode relies on a molecularly well-defined, substrate-coordinating [Ni(SIPr)] unit and is apt for the reduction of internal C=C bonds. The second one rests on the generation of (polynuclear) Ni hydrides that are more suitable for the hydrogenation of terminal alkenes. Both modes do not require any additives (bases, auxiliary hydrides) which renders the catalytic methods atom-efficient and economical.

The fact that the described Ni catalyst also brings about the reduction of ketones and ketimines blazes the trail for the development of new asymmetric hydrogenation catalysts. This and the potential of the Ni–NHC complexes to function as catalysts beyond hydrogenation applications are currently examined in our research laboratories.

Experimental

Catalytic hydrogenation without preactivation (mode I)

In a glovebox, glass vials (4 mL) equipped with a stirring bar were charged with the substrate (0.50 mmol). The respective amount of precatalyst (**[Ni] 4-H**, 1 mol% or as stated) was added as a stock solution. Then, solvent was added until the total volume amounted to 1.0 mL. The vials were closed with a screw cap equipped with a PTFE-coated rubber septum, placed inside an Al inlet, and taken out from the glovebox. Each septum was pierced with a cannula and the vials together with the inlet were placed inside the autoclave which was then flushed with Ar for 15 s, tightly sealed, purged with H_2 (3 × 10 bar, 2 × 20 bar) and pressurized with 20 bar H_2. The thus-prepared steel vessel was then placed into a preheated (45 °C) water bath and the reaction mixture stirred for 3 h. After cooling to room temperature, the overpressure was released and the autoclave was disassembled. The reaction mixtures were analyzed *via* GC-MS. If conversions or yields were determined *via* GC-MS analysis, stock solution of *n*-hexadecane was added after the

reaction. Standard conditions: 1 mol% **[Ni] 4-H**, 1,4-dioxane, 45 °C, 20 bar H_2, 3 h. Deviating reaction conditions and workup methods are described in the supporting information for each substrate.

Catalytic hydrogenation with preactivation (mode II)

The same procedure as was followed for mode I was applied but no substrate was added at first. After preactivation for 3 h at 45 °C under 20 bar H_2, the autoclave was disassembled and the cannulas were quickly removed. Liquid substrates were added through a Hamilton syringe whereas solid substrates were weighed into a separate glass vial in the glovebox. The vials were tightly sealed and then removed from the box. The preactivated catalyst solution was transferred to the substrate-containing vial with a syringe. The septa were then pierced again with cannulas and the autoclave (preheated bottom part at 45 °C) assembled and charged with H_2 according to the standard procedure. The remaining steps were performed as described for mode I. Standard conditions: 1 mol% **[Ni] 4-H**, 1,4-dioxane, 45 °C, 20 bar H_2, and 30 min. Deviating reaction conditions and workup methods are described in the SI for each substrate.

Catalytic hydrogenation of polycyclic aromatic hydrocarbons

The same procedure as delineated for mode I was used. Exact reaction conditions and purification methods are described in the supporting information for each substrate. In most cases, hydrogenation gave at least two products which were not separated during the course of the purification step. Instead, the respective yields were determined by way of ^{1}H NMR spectroscopy using 1,3,5-trimethoxybenzene as internal standard.

Author contributions

S. R.: writing – original draft, methodology, investigation, conceptualization. S. H.: investigation. U. M.: crystal structures. C. T.: writing – review & editing, writing – original draft, validation, supervision, conceptualization.

Conflicts of interest

The authors declare no competing financial interest.

Data availability

All data supporting this article have been included as part of the supplementary information (SI).

Supplementary information: experimental and procedural details, mechanistic studies, NMR spectra (^{1}H, ^{13}C), single crystal X-ray diffraction analyses (tabular information, pictorial representations), HRMS. See DOI: https://doi.org/10.1039/d5cy01341k.

CCDC 2493261–2493267 and 2493739 contain the supplementary crystallographic data for this paper.[78a–h]

Acknowledgements

We gratefully thank Univ.-Prof. Dr. Marko Hapke from the INCA (Linz) for fruitful discussions and the generous support as well as assoc. Univ.-Prof. Dr. Markus Himmelsbach and Laura Zellner MSc from the Institute of Analytical and General Chemistry at the JKU for performing the HRMS measurements.

References

1 H.-J. Arpe, *Industrial Organic Chemistry*, Wiley-VCH, Weinheim, 5th edn, 2010.
2 J. Hagen, *Industrial Catalysis: A Practical Approach*, Wiley-VCH, Weinheim, 3rd edn, 2015.
3 A. Behr, T. Seidensticker and D. Vogt, *Applied Homogeneous Catalysis: A Tool for Sustainable Chemistry*, Wiley-VCH, Weinheim, 2nd edn, 2025.
4 R. M. Bullock, J. G. Chen, L. Gagliardi, P. J. Chirik, O. K. Farha, C. H. Hendon, C. W. Jones, J. A. Keith, J. Klosin, S. D. Minteer, R. H. Morris, A. T. Radosevich, T. B. Rauchfuss, N. A. Strotman, A. Vojvodic, T. R. Ward, J. Y. Yang and Y. Surendranath, *Science*, 2020, **369**, eabc3183.
5 N. A. Eberhardt and H. Guan, *Chem. Rev.*, 2016, **116**, 8373–8426.
6 W. Weigand and P. Schollhammer, *Bioinspired Catalysis: Metal-Sulfur Complexes*, Wiley-VCH, Weinheim, 2015.
7 N. Lalaoui, I. Suarez-Antuna, S. Arjunan, M. Curtil, I. Polydoros-Chrysovalantis, F. Molton, P. Y. Chavant, C. Philouze, A. Milet, P. Maldavi and C. Duboc, *ACS Org. Inorg. Au*, 2025, **5**, 230–237.
8 M. Raney, *US Pat.*, US1563587, 1925.
9 J. Sales, F. Mushtaq, M. D. Christou and R. Nomen, Study of Major Accidents Involving Chemical Reactive Substances: Analysis and Lessons Learned, *Process. Saf. Environ. Prot.*, 2007, **85**, 117–124.
10 Y. Tamaru, *Modern Organonickel Chemistry*, Wiley-VCH, Weinheim, 2005.
11 S. Pisiewicz, D. Formenti, A.-E. Surkus, M.-M. Pohl, J. Radnik, K. Junge, C. Topf, S. Bachmann, M. Scalone and M. Beller, *ChemCatChem*, 2016, **8**, 129–134.
12 P. Ryabchuk, G. Agostini, M.-M. Pohl, H. Lund, A. Agapova, H. Junge, K. Junge and M. Beller, *Sci. Adv.*, 2018, **4**, eaat0761.
13 J. Michalke, K. Faust, T. Bögl, S. Bartling, N. Rockstroh and C. Topf, *Int. J. Mol. Sci.*, 2022, **23**, 8742.
14 Y. Hu, M. Liu, S. Bartling, H. Lund, H. Atia, P. J. Dyson, M. Beller and R. V. Jagadeesh, *Sci. Adv.*, 2023, **9**, eadj8225.
15 J. Michalke, D. Böhm, F. Schmiedbauer, J. F. Schwarz, L. S. Vogl, S. Bartling, N. Rockstroh and C. Topf, *Tetrahedron Green Chem*, 2024, **3**, 100036.
16 X. Cui, Y. Hangkong, K. Junge, C. Topf, M. Beller and F. Shi, *Green Chem.*, 2017, **19**, 305–310.
17 V. Vermaak, H. C. M. Vosloo and A. J. Swarts, *Coord. Chem. Rev.*, 2024, **507**, 215716.
18 H. Itatani and J. C. Bailar, *J. Am. Chem. Soc.*, 1967, **89**, 1600–1602.

19 I. M. Angulo, A. M. Kluwer and E. Bouwman, *Chem. Commun.*, 1998, 2689–2690.
20 I. M. Angulo and E. Bouwman, *J. Mol. Catal. A: Chem.*, 2001, **175**, 65–72.
21 I. M. Angulo, E. Bouwman, R. van Gorkum, S. M. Lok, M. Lutz and A. L. Spek, *J. Mol. Catal. A: Chem.*, 2003, **202**, 97–106.
22 K. V. Vasudevan, B. L. Scott and S. K. Hanson, *Eur. J. Inorg. Chem.*, 2012, **2012**, 4898–4906.
23 Z. Wei, Y. Ren, X. Tian, C. Shen and H. Jiao, *J. Catal.*, 2024, **431**, 115372.
24 J. Wu, J. W. Faller, N. Hazari and T. J. Schmeier, *Organometallics*, 2012, **31**, 806–809.
25 Y. Wang, A. Kostenko, S. Yao and M. Driess, *J. Am. Chem. Soc.*, 2017, **139**, 13499–13506.
26 M.-P. Lücke, S. Yao and M. Driess, *Chem. Sci.*, 2021, **12**, 2909–2915.
27 T. M. Saunders, K. N. Roberston and L. Turculet, *ChemCatChem*, 2024, **16**, e202400654.
28 J. Camacho-Bunquin, M. J. Ferguson and J. M. Stryker, *J. Am. Chem. Soc.*, 2013, **135**, 5537–5540.
29 N. G. Léonard and P. J. Chirik, *ACS Catal.*, 2017, **8**, 342–348.
30 W. H. Harman and J. C. Peters, *J. Am. Chem. Soc.*, 2012, **134**, 5080–5082.
31 T.-P. Lin and J. C. Peters, *J. Am. Chem. Soc.*, 2014, **136**, 13672–13683.
32 R. C. Cammarota and C. C. Lu, *J. Am. Chem. Soc.*, 2015, **137**, 12486–12489.
33 Y. Cai, S. Jiang, T. Rajeshkumar, L. Maron and X. Xu, *J. Am. Chem. Soc.*, 2022, **144**, 16647–16655.
34 Y. Cai, M. Wang, Y. Yang and X. Xu, *Inorg. Chem.*, 2025, **64**, 14598–14605.
35 M. Shevlin, M. R. Friedfeld, H. Sheng, N. A. Pierson, J. M. Hoyt, L.-C. Campeau and P. J. Chirik, *J. Am. Chem. Soc.*, 2016, **138**, 3562–3569.
36 B. Li, Z. Wang, Y. Luo, H. Wei, J. Chen, D. Liu and W. Zhang, *Nat. Commun.*, 2024, **15**, 5482.
37 K. Murugesan, C. B. Bheeter, P. R. Linnebank, A. Spannenberg, J. N. Reek, R. V. Jagadeesh and M. Beller, *ChemSusChem*, 2019, **12**, 3363–3369.
38 N. O. Thiel, B. Kaewmee, T. Tran Ngoc and J. F. Teichert, *Chem. – Eur. J.*, 2020, **26**, 1597–1603.
39 M. L. G. Sansores-Paredes, M. Lutz and M.-E. Moret, *Nat. Chem.*, 2024, **16**, 417–425.
40 D. J. Hale, M. J. Ferguson and L. Turculet, *ACS Catal.*, 2021, **12**, 146–155.
41 T. L. Kalkuhl, I. Fernández and T. J. Hadlington, *Chem*, 2025, **11**, 102349.
42 T. Vielhaber, C. Heizinger and C. Topf, *J. Catal.*, 2021, **404**, 451–461.
43 T. Vielhaber, K. Faust, T. Bögl, W. Schöfberger and C. Topf, *J. Catal.*, 2022, **416**, 352–363.
44 Ł. Banach, P. A. Guńka, J. Zachara and W. Buchowicz, *Coord. Chem. Rev.*, 2019, **389**, 19–58.
45 C. D. Abernethy, A. H. Cowley and R. A. Jones, *J. Organomet. Chem.*, 2000, **596**, 3–5.
46 R. A. Kelly, N. M. Scott, S. Díez-González, E. D. Stevens and S. P. Nolan, *Organometallics*, 2005, **24**, 3442–3447.
47 B. Landers and O. Navarro, *Inorg. Chim. Acta*, 2012, **380**, 350–353.
48 V. Ritleng, C. Barth, E. Brenner, S. Milosevic and M. J. Chetcuti, *Organometallics*, 2008, **27**, 4223–4228.
49 E. Peris, *Chem. Rev.*, 2018, **118**, 9988–10031.
50 A.-J. Arduengo III, R. L. Harlow and M. Kline, *J. Am. Chem. Soc.*, 1991, **113**, 361–363.
51 P. W. N. M. van Leeuwen and J. C. Chadwick, *Homogeneous Catalysts: Activity-Stability-Deactivation*, Wiley, VCH Weinheim, 2011.
52 S. Pelties, D. Herrmann, B. de Bruin, F. Hartl and R. Wolf, *Chem. Commun.*, 2014, **50**, 7014–7016.
53 F. Ulm, Y. Cornaton, J.-P. Djukic, M. J. Chetcuti and V. Ritleng, *Chem. – Eur. J.*, 2020, **26**, 8916–8925.
54 L. P. Bheeter, M. Henrion, L. Brelot, C. Darcel, M. J. Chetcuti, J.-B. Sortais and V. Ritleng, *Adv. Synth. Catal.*, 2012, **354**, 2619–2624.
55 L. P. Bheeter, M. Henrion, M. J. Chetcuti, C. Darcel, V. Ritleng and J.-B. Sortais, *Catal. Sci. Technol.*, 2013, **3**, 3111–3116.
56 F. Ulm, S. Shahane, L. Truong-Phuoc, T. Romero, V. Papaefthimiou, M. Chessé, M. J. Chetcuti, C. Pham-Huu, C. Michon and V. Ritleng, *Eur. J. Inorg. Chem.*, 2021, **30**, 3074–3082.
57 M. G. Avello, S. Golling, L. Truong-Phuoc, L. Vidal, T. Romero, V. Papaefthimiou, N. Gruber, M. J. Chetcuti, F. R. Leroux, M. Donnard, V. Ritleng, C. Pham-Huu and C. Michon, *Chem. Commun.*, 2023, **59**, 1537–1540.
58 M. G. Avello, J. Blas Martínez, T. Romero, V. Papaefthimiou, M. J. Chetcuti, V. Ritleng, C. Pham-Huu, C. Oelschlaeger and C. Michon, *ACS Sustainable Chem. Eng.*, 2024, **12**, 10739–10751.
59 M. G. Avello, G. Singh, L. Truong-Phuoc, L. Vidal, V. Papaefthimiou, M. Chessé, N. Gruber, M. J. Chetcuti, K. Vanka, V. Ritleng, C. Pham-Huu and C. Michon, *J. Catal.*, 2026, **453**, 116487.
60 H. Türkmen, O. Şahin, O. Büyükgüngör and B. Çetinkaya, *Eur. J. Inorg. Chem.*, 2006, **2006**, 4915–4921.
61 S. Redl, D. Timelthaler, P. Sunzenauer, K. Faust and C. Topf, *Organometallics*, 2023, **42**, 1639–1648.
62 O. V. Khazipov, K. E. Shepelenko, D. V. Pasyukov, V. V. Chesnokov, S. B. Soliev, V. M. Chernyshev and V. P. Ananikov, *Org. Chem. Front.*, 2021, **8**, 2515–2524.
63 R. Beck, M. Shoshani and S. A. Johnson, *Angew. Chem., Int. Ed.*, 2012, **51**, 11753–11756.
64 Y. Su, K. Shen, P. Shi, C. Liu, S. Song, H. Yi, A. Lei, Y. Liu, H. Wang, X. Li, Q. Luo, C. Xu and X. Wang, *J. Am. Chem. Soc.*, 2025, **147**, 39561–39571.
65 B. Sawatlon, T. Wititsuwannakul, Y. Tantirungrotechai and P. Surawatanawong, *Dalton Trans.*, 2014, **43**, 18123–18133.
66 Y. Hoshimoto, Y. Hayashi, H. Suzuki, M. Ohashi and S. Ogoshi, *Organometallics*, 2014, **33**, 1276–1282.
67 N. I. Saper, A. Ohgi, D. W. Small, K. Semba, Y. Nakao and J. F. Hartwig, *Nat. Chem.*, 2020, **12**, 276–283.
68 C. Nie, C. Park, J. Kim and P. J. Chirik, *J. Am. Chem. Soc.*, 2024, **146**, 24818–24831.

69 J. Rao, S. Dong, C. Yang, Q. Liu, X. Leng, D. Wang, J. Zhu and L. Deng, *J. Am. Chem. Soc.*, 2023, **145**, 25766–25775.
70 M. P. Williamson, *Prog. Nucl. Magn. Reson. Spectrosc.*, 2013, **73**, 1–16.
71 I. R. Kleckner and M. P. Foster, *Biochim. Biophys. Acta, Proteins Proteomics*, 2011, **1814**, 942–968.
72 M. J. Iglesias, J. F. Blandez, M. R. Fructos, A. Prieto, E. Álvarez, T. R. Belderrain and M. C. Nicasio, *Organometallics*, 2012, **31**, 6312–6316.
73 Y. Zhou, X. Cui, Y. Yang and Z.-Z. Xie, *Organometallics*, 2024, **43**, 987–997.
74 C. Berini, O. H. Winkelmann, J. Otten, D. A. Vicic and O. Navarro, *Chem. – Eur. J.*, 2010, **16**, 6857–6860.
75 J. C. Greenbaum, A. J. King, M. V. Pecoraro, P. Tosatti and K. Puentener, *J. Am. Chem. Soc.*, 2025, **147**, 30423–30435.
76 Y. Hoshimoto, M. Ohashi and S. Ogoshi, *Acc. Chem. Res.*, 2015, **48**, 1746–1755.
77 Y. Cai, L. Ruan, A. Rahman and S. Shi, *Angew. Chem., Int. Ed.*, 2021, **60**, 5262–5267.
78 (*a*) CCDC 2493261: Experimental Crystal Structure Determination, 2025, DOI: 10.5517/ccdc.csd.cc2ppfsm;; (*b*) CCDC 2493262: Experimental Crystal Structure Determination, 2025, DOI: 10.5517/ccdc.csd.cc2ppftn; (*c*) CCDC 2493263: Experimental Crystal Structure Determination, 2025, DOI: 10.5517/ccdc.csd.cc2ppfvp; (*d*) CCDC 2493264: Experimental Crystal Structure Determination, 2025, DOI: 10.5517/ccdc.csd.cc2ppfwq; (*e*) CCDC 2493265: Experimental Crystal Structure Determination, 2025, DOI: 10.5517/ccdc.csd.cc2ppfxr; (*f*) CCDC 2493266: Experimental Crystal Structure Determination, 2025, DOI: 10.5517/ccdc.csd.cc2ppfys; (*g*) CCDC 2493267: Experimental Crystal Structure Determination, 2025, DOI: 10.5517/ccdc.csd.cc2ppfzt; (*h*) CCDC 2493739: Experimental Crystal Structure Determination, 2025, DOI: 10.5517/ccdc.csd.cc2ppy6k.